Monthly Notices
of the
ROYAL ASTRONOMICAL SOCIETY

Mon. Not. R. Astron. Soc. (2010) doi:10.1111/j.1365-2966.2010.17139.x

Recent star formation in local, morphologically disturbed spheroidal galaxies on the optical red sequence

Sugata Kaviraj[1,2,3]★

[1]*Blackett Laboratory, Imperial College London, London SW7 2AZ*
[2]*Mullard Space Science Laboratory, Holmbury St. Mary, Dorking, Surrey RH5 6NT*
[3]*Department of Physics, University of Oxford, Keble Road, Oxford OX1 3RH*

Accepted 2010 June 3. Received 2010 June 3; in original form 2009 June 10

ABSTRACT

We combine *Galaxy Evolution Explorer* [(*GALEX*); ultraviolet (UV)] and Sloan Digital Sky Survey [(SDSS); optical] photometry to study the recent star formation histories of ∼100 field galaxies on the optical red sequence, a large fraction of which exhibit widespread signs of disturbed morphologies in deep optical imaging that are consistent with recent merging events. More than 70 per cent of bulge-dominated galaxies in this sample show tidal features at a surface brightness limit of $\mu \sim 28\,\mathrm{mag\,arcsec^{-2}}$. We find that, while they inhabit the optical red sequence, they show a wide spread in their UV colours (∼4 mag), akin to what has been discovered recently in the general early-type population. A strong correlation is found between UV colour and the strength of the tidal distortions, such that the bluest galaxies are more distorted. This strongly suggests that the blue UV colours seen in many nearby early types are driven by (low-level) merger-induced star formation within the last 3 Gyrs, contributing less than 10 per cent of the stellar mass. If the ongoing mergers in this sample, which have a median mass ratio of 1:4, are representative of the nearby red merger population, then less than ∼25 per cent of the new stellar mass in the remnants is typically added through merger-induced star formation. While the dust extinction in the interstellar medium (ISM) in these galaxies is small ($E^{\mathrm{ISM}}_{B-V} < 0.1$), the local dust content of the star-forming regions is, on average, a factor of ∼3 higher. Finally, we use our theoretical machinery to provide a recipe for calculating the age of the most recent star formation event (t_2) in nearby ($z \lesssim 0.1$) red early-type galaxies: $\log t_2(\mathrm{Gyrs}) \sim 0.6^{\pm 0.03}\,[(\mathrm{NUV} - u) - (g - z) - 1.73^{\pm 0.03}]$, where NUV, u, g and z are the observed photometric magnitudes of the galaxies in the *GALEX*/SDSS filter sets.

Key words: galaxies: elliptical and lenticular, cD – galaxies: evolution – galaxies: interactions – galaxies: starburst.

1 INTRODUCTION

The formation histories of luminous, spheroidal galaxies have posed a serious challenge to models of galaxy formation for the last few decades. The classical 'monolithic collapse' hypothesis, that followed the model of Eggen, Lynden-Bell & Sandage (1962) for the formation of the Galaxy (e.g. Larson 1974; Chiosi & Carraro 2002), postulated that stellar populations in early-type galaxies form in short, highly efficient starbursts at high redshift ($z \gg 1$) and evolve purely passively thereafter. Indeed, the optical properties of the early-type population and their strict obedience to simple scaling relations are remarkably consistent with such a simple formation scenario. The small scatter in the early-type 'Fundamental Plane' (e.g. Jorgensen, Franx & Kjaergaard 1996; Saglia et al. 1997) and its apparent lack of evolution with look-back time (e.g. Franx 1993, 1995; van Dokkum & Franx 1996; Forbes, Ponman & Brown 1998; Peebles 2002), the homogeneity and lack of redshift evolution in their optical colours (e.g. Bower, Lucey & Ellis 1992; Bender 1997; Ellis et al. 1997; Stanford, Eisenhardt & Dickinson 1998; Gladders et al. 1998; van Dokkum et al. 2000) and evidence for short (<1 Gyrs) star formation time-scales in these systems, deduced from the overabundance of α elements (e.g. Thomas, Greggio & Bender 1999), all suggest that the bulk of the stellar population in early-type galaxies does indeed form at high redshift ($z > 2$).

Nevertheless, consensus, in recent years, has moved away from monolithic collapse towards a more gradual assembly of these systems in the framework of the standard Λ cold dark matter (ΛCDM)

★E-mail: s.kaviraj@imperial.ac.uk

galaxy formation paradigm. Following the seminal work of Toomre (1977), numerical simulations have consistently demonstrated that galaxy collisions end in rapid merging – a fundamental feature of the standard model – and typically produce spheroidal remnants (e.g. Barnes & Hernquist 1992) in cases where the mass ratios of the progenitors are large ($\geq$1:3). Semi-analytical models of galaxy formation, that incorporate these results, have had reasonable success in reproducing the morphological mix of the Universe and the (photometric) properties of the early-type population (e.g. Cole et al. 2000; Hatton et al. 2003; Kaviraj et al. 2005; De Lucia et al. 2006). The predicted star formation histories (SFHs) of early-type galaxies (at least in clusters) in the semi-analytical framework have been shown to be quasi-monolithic, resulting in good agreement with the optical colours and their evolution with redshift (Kaviraj et al. 2005). As a result, the observed optical properties of the early-type population and their consistency with the expectations of monolithic collapse are not proof of a uniquely monolithic origin.

A drawback of optical data is its relative insensitivity to small amounts of recent star formation (RSF). The optical spectrum remains largely unaffected by the minority of stellar mass that is expected to form in these systems at low and intermediate redshifts ($z < 1$), which makes it difficult to accurately measure early-type SFHs over the last eight billion years. However, while it does not impact the optical spectrum (within typical observational and theoretical uncertainties), a small mass fraction (a few per cent) of young (a few tens of Myr old) stars strongly affects the rest-frame ultraviolet (UV) spectrum shortward of 3000 Å. Furthermore, the UV remains largely unaffected by the age–metallicity degeneracy (Worthey 1994) that plagues optical analyses (Kaviraj et al. 2007a), making it an ideal photometric indicator of RSF. The advent of the *Galaxy Evolution Explorer* (*GALEX*) space telescope (Martin et al. 2005) has provided us with an unprecedented opportunity to harness the sensitivity of the UV to young stars to quantify the presence of RSF in local early-type galaxies. Following the early work of Yi et al. (2005), Kaviraj et al. (2007b, hereafter K07), Schawinski et al. (2007a) and Kaviraj et al. (2008) have carefully studied the UV properties of the early-type population at late epochs (see Kaviraj 2008 for a review), to convert the UV flux observed in these systems into a measurement of the RSF, taking into account potential contributions to the UV spectrum from old, evolved stellar stages such as horizontal branch (HB) stars. It is worth noting that models where early-types host only old stars with realistic metallicity distributions that satisfy both the mean metallicity and α-enhancements of nearby early-types clearly require RSF (see section 6.2 in K07). These results indicate that early types of all luminosities form stars over the lifetime of the Universe, with massive systems accumulating 10–15 per cent of their stars since $z \sim 1$, plausibly through minor mergers with small, gas-rich companions (Kaviraj et al. 2009).

While such recent efforts have made a compelling case for RSF-driven UV excess in the early-type population, we should note some caveats to this analysis. The contamination of the UV spectrum by old HB stars is a possibility at low redshift, especially in giant elliptical galaxies (see e.g. Yi, Demarque & Oemler 1997; Yi et al. 1999). However, studies of the rest-frame UV at high redshift ($z >$ 0.5), where the HB is absent, reveal a similarly large scatter in the rest-frame UV colour–magnitude relation (CMR) to what is observed in the nearby Universe, strongly suggesting that the principal drivers of the UV excess are not HB stars (Kaviraj et al. 2008). It is conceivable that there is some contribution to the UV flux from alternative hot stellar populations such as blue stragglers – stars found above the turn-off in Hertzprung–Russell diagrams (Wheeler 1979) – typically within old globular clusters (GCs). Since they are likely to form through stellar interactions (Mapelli et al. 2006), these objects tend to inhabit the cores of GCs, where the stellar density is high. However, GCs (to which their constituent blue stragglers contribute a vanishing fraction of stellar mass) host a small fraction of the total stellar mass in the galaxy, making it unlikely that the blue straggler population are responsible for the UV flux in elliptical galaxies (Mochkovitch 1986).

We note that such alterative contributions to the UV flux in early-type galaxies have not been fully explored in the context of contemporary rest-frame UV data from *GALEX* at low redshift and deep optical surveys at high redshift. While RSF provides the most attractive solution, both in terms of the observed UV spectra of individual galaxies and in the context of the currently accepted galaxy formation paradigm, the (presumably minor) role of these alternate sources of UV flux remains an open question. A potentially robust discriminant between RSF and old stars is the spatial distribution of UV flux in the galaxy. If it is dominated by old stars (e.g. HB stars), the UV light is expected to be a smooth background, perhaps with a colour gradient (due to metallicity variations across the galaxy), but without large pixel-to-pixel variations or pronounced fine structure. A firm understanding of the origin of the UV flux would greatly benefit from high-resolution imaging of nearby early types, e.g. using forthcoming instruments such as the *Hubble Space Telescope* (*HST*)-Wide Field Camera 3 (WFC3).

In this work, we study the *GALEX* (UV) and Sloan Digital Sky Survey (SDSS; optical, see Adelman-McCarthy et al. 2006) properties of early-type galaxies on the optical red sequence, originally studied by van Dokkum (2005, hereafter vD05). The novelty of the vD05 study was the unprecedented depth of the optical imaging employed to study the red galaxy population. Using $\sim$27 000-s exposures on 4-m class telescopes (equivalent to $\sim$20 h on a 2.5-m class telescope like the one used for the SDSS) vD05 found widespread signatures of recent merging in a large fraction of their early-type sample – more than 70 per cent of bulge-dominated (E/S0) galaxies on the optical red sequence exhibit distorted morphologies, with predominantly red tidal features that extend to spatial scales $>$50 kpc. The deep images allow a quantitative measure of the perturbed morphologies of nearby early-type systems, which is not possible with the substantially shallower imaging offered by other surveys on 1–2.5 m telescopes. As an example, the effective exposure time of the SDSS – on which most of the recent early-type efforts are based – is only $\sim$51 s in each filter (York et al. 2000).

GALEX UV imaging of the vD05 sample provides a unique opportunity to study the SFH of systems that are, to high confidence, recent merger remnants. We first establish that the vD05 sample is representative of the general luminous red galaxy population at similar redshifts. We then combine the *GALEX*/SDSS photometry of the vD05 sample to quantify the RSF in these systems and explore the correlations between (NUV $-$ r), the derived SFHs and the strength of the tidal distortions. Finally, we use our theoretical machinery to derive a simple recipe to translate the observed NUV and optical colours of local early-type galaxies into an estimate of the age of the last star formation episode in these galaxies.

2 THE GALAXY SAMPLE

The original red galaxy sample of vD05 was selected from two deep extragalactic surveys: the Multiwavelength Survey by Yale–Chile (MUSYC; Gawiser et al. 2006) and the NOAO Deep Wide-Field Survey (NDWFS; Jannuzi et al. 1999). The combined data set covers 10.5 deg^2 of sky, reaching 1σ surface brightness

levels of $\mu \sim 29\,\mathrm{mag\,arcsec^{-2}}$. We refer readers to section 3 of vD05 for a comprehensive description of the data set.

For the purposes of this study the vD05 sample was cross-matched with both the SDSS Data Release 4 (DR4) and *GALEX* GR2.[1] Out of the original 126 galaxies in the vD05 sample, the cross-matching process yields 101 galaxies with both *GALEX* and SDSS photometry. The galaxies in this sample have a mean redshift of $z \sim 0.11$. The early-type galaxies, that form the focus of this study, typically have super-L^* luminosities ($M_r^* \sim -21.15$ in the nearby Universe; see Bernardi et al. 2003) and their masses range between $10^{10.4}$ and $10^{11.6}\,\mathrm{M}_\odot$.

Finally, we note that vD05 provides a quantitative measure of the tidal distortions in each object by comparing galaxy images to elliptical galaxy models, generated using the ELLIPSE task in IRAF (see section 5.3 in vD05 for a description of the procedure). This tidal parameter (denoted by T in this paper) measures the median absolute deviation of the (fractional) residuals from the model fit. Comparison of the value of T to visual inspection of the galaxy images indicates that, $T \leq 0.08$ in galaxies where the distortions are not obvious to the eye, $0.13 \leq T \leq 0.19$ for weakly disturbed systems and $T \geq 0.19$ for systems that show strong tidal distortion. The maximum value of the tidal parameter in this sample is ∼0.47. In the following sections, we use this tidal parameter to represent the extent of the morphological disturbance in each galaxy.

3 EMISSION-LINE PROPERTIES, SPATIAL DISTRIBUTIONS AND UV–OPTICAL COLOURS

3.1 Emission-line properties: AGN and star formation activity

The SDSS spectra of individual galaxies were used to determine the presence of Type II active galactic nucleus (AGN) from optical emission-line ratios, using a 'BPT'-type (e.g. Baldwin, Phillips & Terlevich 1981) analysis.

In Fig. 1, we present the BPT plot for the vD05 sample. Grey dots indicate the AGN population in the low-redshift Universe, extracted by Kauffmann et al. (2003). Large circles denote galaxies in the vD05 sample. Galaxies are shown using filled circles if all four emission lines have signal-to-noise ratio S/N > 3. Galaxies where only [N II] and Hα are detected are shown using open circles. Note that while the detection of [N II] and Hα allows us to classify these galaxies as AGN, the type of the AGN remains unclear, since the position on the y-axis depends on the strength of [OIII] and Hβ which are not robustly detected.

It is remarkable that only two of the galaxies lie close to the 'star-forming' sequence of Kauffmann et al. (which is demarcated by the solid curve in the BPT plot). This is strong evidence that the red mergers in vD05 are indeed mostly 'dry' and are not accompanied by significant ongoing star formation (see also Whitaker & van Dokkum 2008). The AGN fraction in this sample is ∼11 per cent, consistent within errors (∼ ± 3 per cent) with the fraction found in the general early-type population (15 per cent) drawn from the entire SDSS at low redshift (e.g. Schawinski et al. 2007b). It is also worth noting that most of the AGN in this sample are classified as Low-Ionization Nuclear Emission-Line Regions (LINERs). A significant fraction of these systems could, in fact, be systems with declining star formation, where the 'LINER-like' emission is driven by post-asymptotic giant branch stars and white dwarfs (see Stasińska et al. 2008). While further exploration of this issue is beyond the scope of this paper, we do not find compelling evidence of strong AGN activity in the vD05 sample.

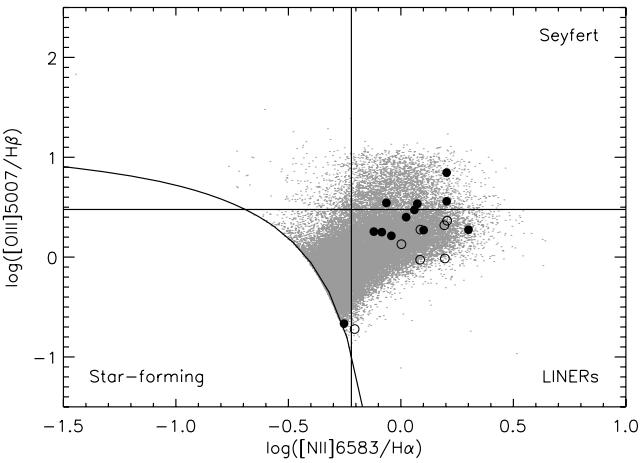

Figure 1. A 'BPT'-type plot for the vD05 red galaxy sample, which indicates that only two galaxies lie near the star-forming sequence and that the bulk of the emission-line activity is LINER like. The grey dots indicate the AGN population in the low-redshift Universe, studied by Kauffmann et al. (2003). The large circles denote galaxies in the vD05 sample. Galaxies are shown using filled circles if all four lines have S/N > 3. Galaxies where only the [N II] and Hα are detected are shown using open circles.

3.2 Spatial distributions and UV–optical colours

We begin by studying some basic properties of the vD05 objects. Fig. 2 indicates the spatial coordinates (RA, Dec. and redshift) of the galaxy sample (top) and its redshift distribution (bottom). Symbol sizes are proportional to the tidal parameter described in Section 2. Galaxies that contain active AGN are shown using open symbols and objects that are currently interacting are indicated using boxes. The redshifts of the galaxies in the top panel of this figure are shown colour coded. We also indicate the angular sizes, at $z = 0.1$ and 0.05, of a 3-Mpc structure (similar to the extent of the Coma cluster).

Given the high incidence of tidal features in the vD05 early-type sample, we first check the spatial distribution of the objects to look for particular overdensities that might lead to the observed high frequency of interactions in the sample. The vD05 study did not consider the spatial distribution of the galaxy sample due to a lack of redshifts. They did estimate, however, that the median redshift of the galaxies was $z \sim 0.1$, based on the optical ($B - R$) colour of an L^* elliptical galaxy. Based on the spectroscopic redshifts from the SDSS (bottom panel of Fig. 2) we find that the mean redshift of this sample to be ∼0.11, in good agreement with the value estimated by vD05.

We find that the sample occupies three main redshift peaks. Note, however, that the redshift binning used in Fig. 2 is $\delta z = 0.01$ – which translates to a distance of ∼50 Mpc at $z = 0.1$ in the standard cosmology – and that the peaks have widths of at least $\delta z = 0.02$. Given the high accuracy of the SDSS redshifts ($\sim 10^{-4}$), the redshift distribution does not indicate that the galaxies are part of structures as compact as cluster cores (which are sub-Mpc structures). Furthermore, the transverse distances (in RA and Dec.) are also quite large compared to, for example, the full extent of the Coma cluster (3 Mpc). Given that the central regions of nearby clusters are

[1] The positional matching with *GALEX* was performed within a 4-arcsec radius – the fiducial *GALEX* point spread function (PSF) is 6 arcsec.

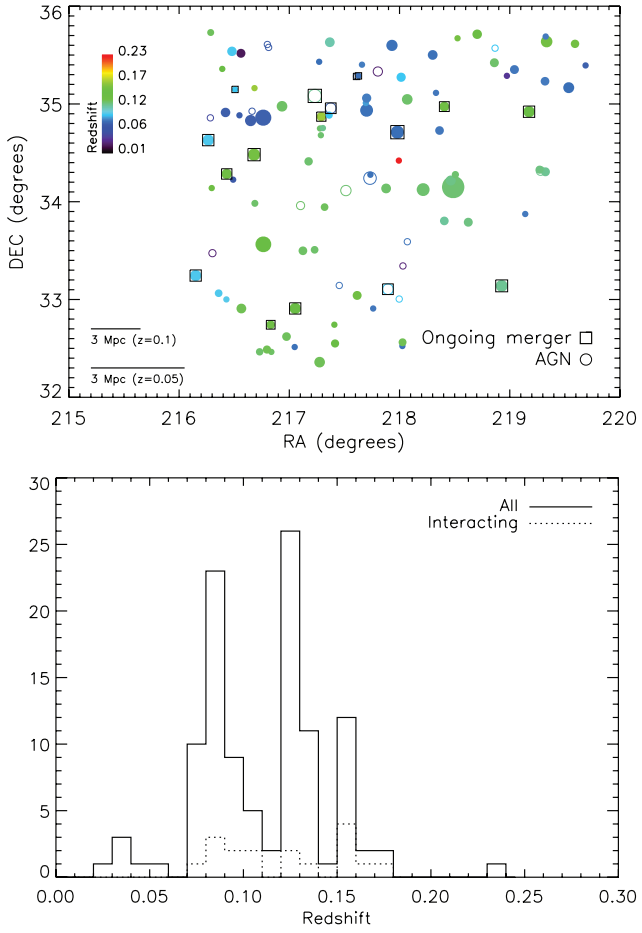

Figure 2. Top: spatial coordinates (RA, Dec. and redshift) of the galaxy sample studied here. Bottom: comparison of the redshift distribution of the general galaxy sample to that of only the interacting population. Our results indicate that the vD05 galaxies are generally in the 'field'. Symbol sizes are proportional to the tidality parameter described in Section 2. Galaxies with active AGN are shown using open symbols and objects that are currently interacting are indicated using boxes. Open boxes indicate ongoing mergers with AGN activity. We also indicate the angular sizes, at $z = 0.1$ and 0.05, of a 3-Mpc structure (similar to the extent of the Coma cluster). The redshift binning in this plot is $\delta z \sim 0.01$, which translates to a distance of ∼50 Mpc at $z = 0.1$ in the standard cosmology.

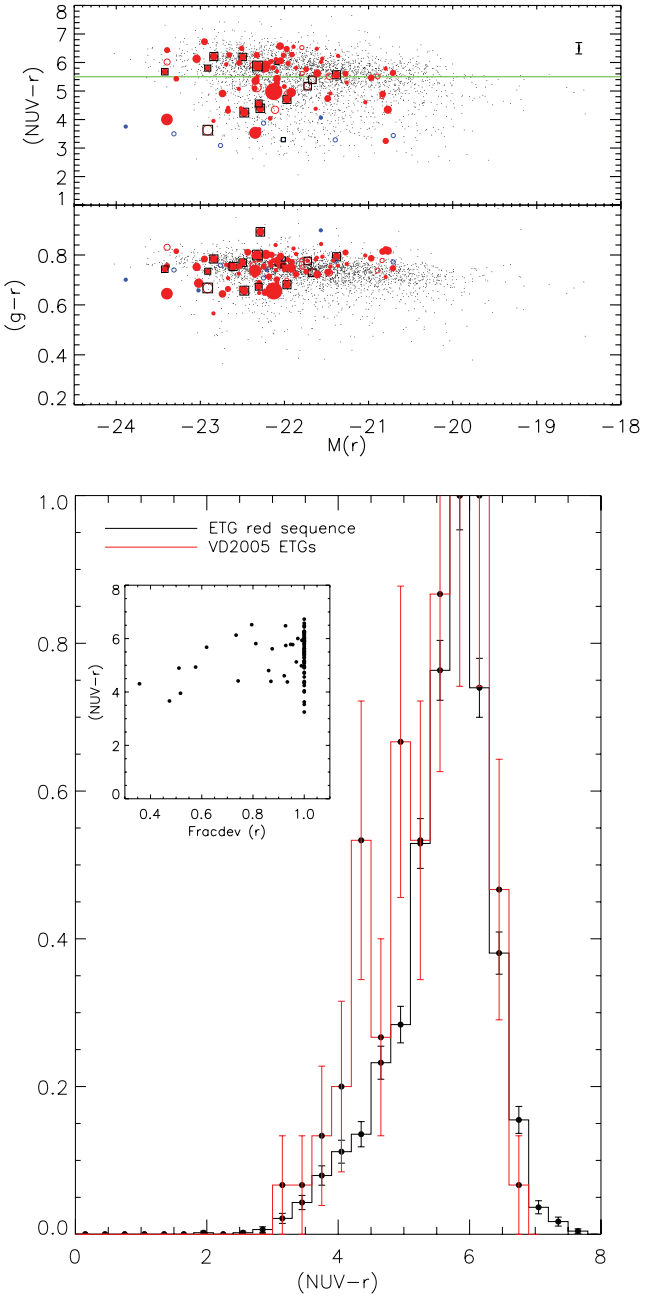

Figure 3. Top: the optical and UV CMRs. While selected to be optically red, the vD05 sample has a large range of UV colours. Red symbols indicate early-type galaxies while blue symbols indicate spirals. Symbol sizes are proportional to the tidal parameter described in Section 2. Galaxies that contain active AGN are shown using open symbols and objects that are currently interacting are indicated using boxes. Small black dots indicate the nearby ($0 < z < 0.1$), massive ($> L^*$) early-type population drawn from the SDSS following the method used by K07. Galaxies blueward of (NUV $- r$) ∼ 5.5 (indicated using the green horizontal line) are very likely to have had some star formation within the last Gyrs (see section 3 in K07). Bottom: comparison between the UV colours of the general early-type population on the optical red sequence ($g - r > 0.65$) and the vD05 sample. See text for more discussion.

dominated by red galaxies (Dressler 1980), we do not find compelling evidence for the vD05 sample to be drawn out of a small number of overdense regions. The galaxies therefore appear to be, on average, in the 'field'.

The top panel of Fig. 3 shows the UV and optical CMRs for the vD05 objects. Small black dots indicate the nearby ($0 < z < 0.1$), massive ($> L^*$) early-type population, drawn from the SDSS DR4 following the method used by K07. Briefly, early-type galaxies are selected from the SDSS using the pipeline parameter 'fracdev', which provides a probabilistic measure of how well a 'de Vaucouleurs' profile fits the galaxy's light profile. Galaxies with fracdev >0.95 are extracted and then visually inspected to remove contaminants such as face-on spirals. Galaxies blueward of (NUV $- r$) ∼ 5.5 (indicated by the green horizontal line) are very likely to have had some star formation within the last Gyrs (see section 3 in K07). It is clear that, while the galaxies in this sample are optically red, they exhibit a wide spread in UV colours.

We note that a central AGN could contaminate the UV spectrum of a galaxy, perhaps enhancing the blue UV colour. However, the contamination from a Type II AGN is likely to be less than around 15 per cent in UV flux, which translates to around 0.15 mag in the

(NUV − r) colour, much smaller than the spread in the UV CMR (∼6 mag; see Salim et al. 2007). Typically, blue early-type colours (NUV − r < 5.5) are not restricted to galaxies hosting AGN, either in the sample studied here or in the general early-type population studied by K07. Furthermore, the quality of the SED fitting that is used to calculate SFHs (see the next section) is equally good in galaxies which carry BPT signatures of AGN and those that do not show any signs of AGN, indicating that there is no measurable contribution from a power-law component. Finally, a study of the *GALEX* images of nearby AGN hosts indicates that the UV emission is extended, making it unlikely that it comes from a central source (Kauffmann et al. 2007). Thus, the presence of Type II AGN does not affect the analysis in this paper.

We begin by comparing the vD05 galaxies to the general early-type population. For a direct comparison we restrict the analysis to the K07 optical red sequence ($g - r > 0.65$) in the redshift range $0.05 < z < 0.1$ and compare the UV colour distribution of the two samples (bottom panel of Fig. 3). We find that the UV distributions are consistent with each other (within counting errors), although the vD05 sample does show a slight excess of objects in two intermediate colour bins around (NUV − r) ∼ 4.3 and (NUV − r) ∼ 4.7.

Recall, however, that the method for selecting the general early-type galaxy population in K07 involves extracting galaxies whose light profiles in the g, r and i bands match a 'de Vaucouleurs' profile very closely (by setting fracdev > 0.95 when selecting objects from the SDSS data base). To quantify the effect of this criterion on the colour comparison, we study the variation of the (NUV − r) colour in the vD05 sample with their fracdev values (inset in the bottom panel of Fig. 3). About 57 per cent of the vD05 galaxies with fracdev < 0.95 have (NUV − r) < 5. The fraction of early types that were missed from K07 as a result of the fracdev > 0.95 criterion is around 20 per cent, from early-type catalogues selected by eye inspection alone (i.e. no fracdev cut; Schawinski, private communication). Assuming a red sequence fraction of ∼70 per cent (since K07 estimated that 30 per cent of the early-type population were blue) implies an ∼8 per cent (57 × 20 × 70 per cent) increase in the fraction of general early types with colours blueward of NUV − r ∼ 5.

This correction removes most of the discrepancy in the UV colour distributions. However, the fraction of objects in the colour bin around (NUV − r) ∼ 4.3 remains inconsistent within 1σ uncertainties, although the histograms are consistent at the 2σ level. A simple Kolmogorov–Smirnov (KS) test (see e.g. Wall 1996) indicates that the probability that the two populations are drawn from the same parent distribution is ∼72 per cent. A similar conclusion is drawn if we use a Kuiper test (which maintains sensitivity near the tails). Thus, we find good overall agreement between the colour distributions, with the difference plausibly caused by cosmic variance, since the sky coverage of the SDSS DR4 (from which the early-type population is derived) is more than two orders of magnitude larger than that of the vD05 sample.

3.3 Correlation between colour and tidal distortion

In Fig. 4, we plot the UV and optical colours against the tidal parameter. Note that the vertical scale in the top panel of this figure, which shows the (NUV − r) colour, spans 4 mag, while that for the ($g - r$) colour spans only 0.3 mag. We explore the strength of the correlation between colour and tidal distortion using Spearman's rank correlation test, which produces a non-parametric measure (ρ) of the statistical dependence between two variables. The value of

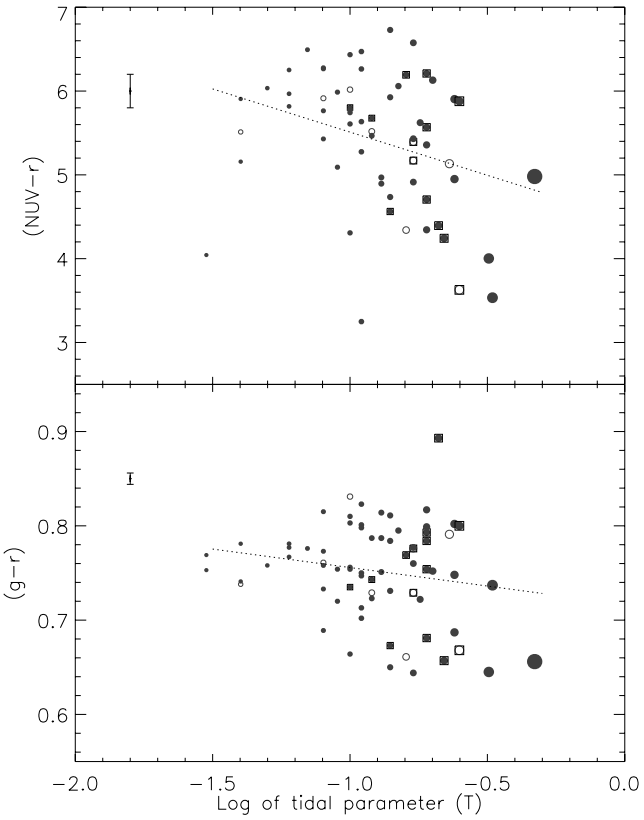

Figure 4. Tidal parameter plotted against (NUV − r) and ($g - r$) colours. A statistically significant correlation exists between the tidal parameter and both the UV and optical colours (see text in Section 3.3 for details). The symbol size scales with the size of the tidal distortion. Galaxies that host Type II AGN are shown using open symbols. Bluer galaxies show higher tidal distortions, with the trend being much stronger in the (NUV − r) colour, due to its higher sensitivity to small amounts of recent star formation.

ρ varies between +1 and −1, which indicate perfect positive and negative correlations, respectively. $\rho \sim 0$ indicates a complete lack of correlation between the variables.

We find that, for the relationship between (NUV − r) and the tidal parameter, $\rho = -0.43$. The significance of this value is 0.0032. This is the probability of finding a correlation between (NUV − r) and the tidal parameter purely through statistical accident. Since this number is very small, this implies that the correlation is statistically significant. The corresponding values for the ($g - r$) colour are $\rho = -0.08$, with a significance of 0.35. Note that the probability of a chance correlation is higher for the optical colour essentially due to the correlation being weaker. We find, therefore, that a measurable correlation exists between both the optical and UV colours and tidal distortion in the galaxy. Not unexpectedly, the correlation is much stronger (and has higher confidence) in the UV colour, since it is much more sensitive to small amounts of RSF.

The reasonably large scatter in the relationship between colour and tidal distortion can be understood by noting that the stellar populations that are responsible for the tidal features and those that drive the UV colours tend to be different. Assuming that the RSF is driven by merging (see also Kaviraj et al. 2010), numerical simulations (e.g. Kaviraj et al. 2009; Peirani et al. 2010) indicate that the tidal features form from the underlying stellar populations of the accreted satellite, while the UV colour is sensitive to the gas content of the satellite and how far star formation has progressed when the remnant is viewed. For example, two satellites with similar

underlying stellar populations but different gas contents might yield similar tidal distortions (if viewed at the same point during the merger process) but exhibit different UV colours. Thus, while a high tidal distortion should, in general, be expected to coincide with a blue UV colour because the remnant is viewed at an earlier phase in the merger/star formation process and the stellar populations are younger, the spread in the satellite gas contents will induce a scatter into the correlation.

4 RECENT STAR FORMATION HISTORIES

4.1 Parameter estimation

A key objective of this work is to quantify the RSF in the vD05 sample. We are primarily interested in exploring the age of the last star formation event (which is presumably linked to the morphological disturbances observed in the deep optical images) and the stellar mass fractions contributed by these events.

We estimate parameters governing the SFH of each galaxy by comparing its (FUV, NUV, u, g, r, i, z) photometry to a library of synthetic photometry, generated using a large collection of model SFHs, specifically optimized for studying spheroidal galaxies at low redshift. As we describe below, our scheme decouples the RSF episode from the star formation that creates the bulk, underlying population. We choose a parametrization for the model SFHs that both minimizes the number of free parameters and captures the macroscopic elements of the SFH of spheroidal galaxies in the low-redshift Universe.

Since the underlying stellar mass in spheroidals forms at high redshift and over short time-scales, we model the underlying stellar population using an instantaneous burst at high redshift. We put this first (primary) instantaneous burst at $z = 3$. Note that changing this to $z = 2$, or even $z = 1$, does not affect our conclusions about the RSF, because the first burst does not contribute to the UV. A large body of recent evidence suggests that the star formation in these systems in the nearby Universe is driven by minor mergers (see Kaviraj et al. 2010, and references therein). This star formation is bursty and we model the RSF episode using a second instantaneous burst, which is allowed to vary in age between 0.001 Gyrs and the look-back time corresponding to $z = 3$ in the rest frame of the galaxy, and in mass fraction between 0 and 1. Our parametrization is similar to previous ones used to study elliptical galaxies at low redshifts (e.g. Ferreras & Silk 2000). We briefly note that our scheme differs in construction from other recent work that explores the general galaxy population at higher redshifts, without reference to morphology (e.g. Muzzin et al. 2009). In particular, the decoupling employed in this study between RSF and the bulk stellar population is difficult to apply at high redshift, where the underlying stellar populations are actively being assembled. Thus, our particular parametrization works best in spheroidal galaxies at low redshift and is not directly comparable to more general schemes, especially in the high-redshift regime.

To build the library of synthetic photometry, each model SFH is combined with a single metallicity in the range 0.1 to 2.5 $Z_{\odot}$ and a value of dust extinction parametrized by E_{B-V} in the range 0 to 0.5. The dust model employed in this study is the empirical dust prescription of Calzetti et al. (2000). Photometric predictions are generated by combining each model SFH with the chosen metallicity and E_{B-V} values and convolving with the stellar models of Yi (2003) through the *GALEX* and SDSS filter sets. The model library contains ∼750 000 individual models. Note that the FUV and NUV filters have effective wavelengths of ∼1500 and ∼2300 Å, respectively.

Since our galaxy sample spans a range of redshifts, equivalent libraries are constructed at redshift intervals of $\delta z = 0.01$. A fine redshift grid is essential in such a low-redshift study because a small change in redshift produces a relatively large change in look-back time over which the UV flux can change substantially, inducing '*K*-correction-like' errors into the analysis.

The primary free parameters in this analysis are the age (t_2) and mass fraction (f_2) of the second burst (the mass fraction of the primary burst is simply $1 - f_2$). Secondary parameters of interest are the dust properties of the system. In particular, the dust content of the primary burst, $E^{\rm PB}_{B-V}$ (which is effectively tracing the 'underlying' population of the galaxy), should provide a measure of the extinction in the interstellar medium (ISM), while the dust in the secondary burst ($E^{\rm SB}_{B-V}$) should reflect the dust in the star formation regions and their vicinity.

In each case, the values of the free parameters are estimated by comparing each observed galaxy to every model in the synthetic library, with the likelihood of each model ($\exp - \chi^2/2$) calculated using the value of χ^2, computed in the standard way. In addition to the observational errors for each object, we assume additional uncertainties that account for uncertainties in the models (e.g. Yi 2003), model offsets from observational data (e.g. Eisenstein et al. 2001; Maraston et al. 2009) and systematic errors in *GALEX* and SDSS photometry (see e.g. Ivezić et al. 2004; Morrissey et al. 2007). These are taken to be 0.05 mag for the optical filters, 0.2 mag in FUV and 0.1 mag for the NUV passband. The two types of uncertainty are added in quadrature. From the joint probability distribution, each parameter is marginalized to extract its one-dimensional probability density function (PDF). We take the median of this PDF as the best estimate of the parameter in question and the 16 and 84 percentile values as the '1σ' uncertainties on this estimate. In the analysis that follows we present these median parameter values.

The leverage in t_2 and the quality of the t_2 fits depends critically on our access to the rest-frame UV, which hosts most of the flux from hot, young main-sequence stars. Note that Whitaker & van Dokkum (2008) have demonstrated that the spheroidal galaxies in the vD05 sample are virtually dustless, so that there should be very little reprocessing of the UV–optical light into the infrared passbands. Muzzin et al. (2009) have shown that the inclusion of rest-frame near-infrared (NIR) filters does not alter the mean values of fitted parameters (although they do reduce the derived uncertainties) for galaxies in the high-redshift ($z \sim 2$) Universe, which should be significantly dustier than our low-redshift spheroidal sample. Since our sample is dust poor, it seems reasonable, therefore, to suggest that the addition of NIR filters will leave our conclusions regarding the derived parameters unchanged. Finally, a similar analysis on a small sample of SDSS early-type galaxies which have, in addition to *GALEX*, NUV photometry from the *XMM* Optical Monitor (OM; the OM has three NUV filters around *GALEX* NUV; see Mason et al. 2001) indicates that a larger number of UV filters leaves the median values of t_2 and f_2 unchanged, with the uncertainties decreasing by ∼10 per cent. Thus the size of our filter set, both in the UV and in the optical spectrum, is optimal for the aims of this paper.

4.2 Star formation history parameters

4.2.1 Age and mass fraction of the second burst

Fig. 5 shows the age (t_2) and mass fraction (f_2) of the RSF estimated to have formed in the second burst in each of the vD05 early types. Galaxies are colour coded based on their (NUV − r) colour and average uncertainties in the parameters are indicated in the plot.

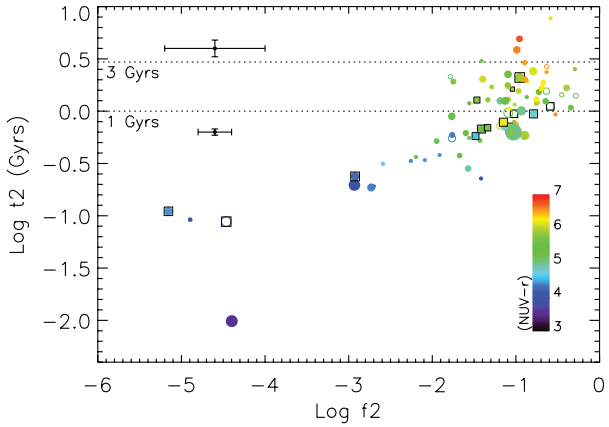

Figure 5. Ages (t_2) and mass fractions (f_2) of the second star formation episode in the early-type galaxies studied here. The bulk of the vD05 sample has experienced a star formation event in the last 3 Gyrs, which typically adds less than 10 per cent to the stellar mass of the galaxy. Symbol sizes are proportional to the tidal parameter described in Section 2. Galaxies that contain active AGN are shown using open symbols and objects that are currently interacting are indicated using boxes. The galaxies are shown colour coded based on their (NUV − r) colour.

Note that although the UV colour changes rapidly with the value of t_2, the same colour can be degenerate with a wide range of mass fractions f_2 (see fig. 1 in Kaviraj 2008). Since this effect becomes more pronounced as the starburst ages, the mass fraction errors become larger at higher ages. As a result, while we can typically constrain the age of the second burst with good accuracy, the uncertainty in the mass fraction could span almost a decade.

We find that the bulk of the objects in our sample have experienced a star formation event in the last 3 Gyrs. Considering galaxies which have well-constrained mass fraction uncertainties, the median values of f_2 are typically less than 10 per cent. 5 per cent of the early-type sample has experienced a star formation event within the last 0.1 Gyrs. The very low mass fractions in this subset may indicate that the star formation in these events is still ongoing.

Note that the median mass ratio of the ongoing mergers in the vD05 sample is 1:4. If the ongoing mergers are representative of the red merger population, then less than 25 per cent of the new stellar mass in the remnants is contributed by star formation. The rest is 'dry accretion' of existing stars in the progenitor galaxies. Note, however, that the errors in the mass fraction estimates are typically quite large and this statement probably carries with it some uncertainty. Using the lower limit of the error bars in the mass fraction would suggest a lower fraction of less than 10 per cent being contributed by star formation, which is consistent with the recent literature (e.g. van Dokkum et al. 2010).

In Fig. 6, we plot the age (t_2) and mass fraction (f_2) of the second burst against the tidal parameter. Recall that t_2 is effectively the look-back time to the last star formation event in the galaxy. We find that galaxies with larger tidal distortions show lower values of t_2, consistent with the expectation that the intensity of the tidal distortion decreases with time, resulting in the observed correlation between the tidal parameter and t_2. The best-fitting relation is described by

$$\log T \sim -0.91^{\pm 0.03} - 0.21^{\pm 0.05} \log t_2\,(\mathrm{Gyrs}). \quad (1)$$

A weaker correlation is found between the mass fraction formed in the recent starburst (f_2) and the tidal parameter, as shown in the

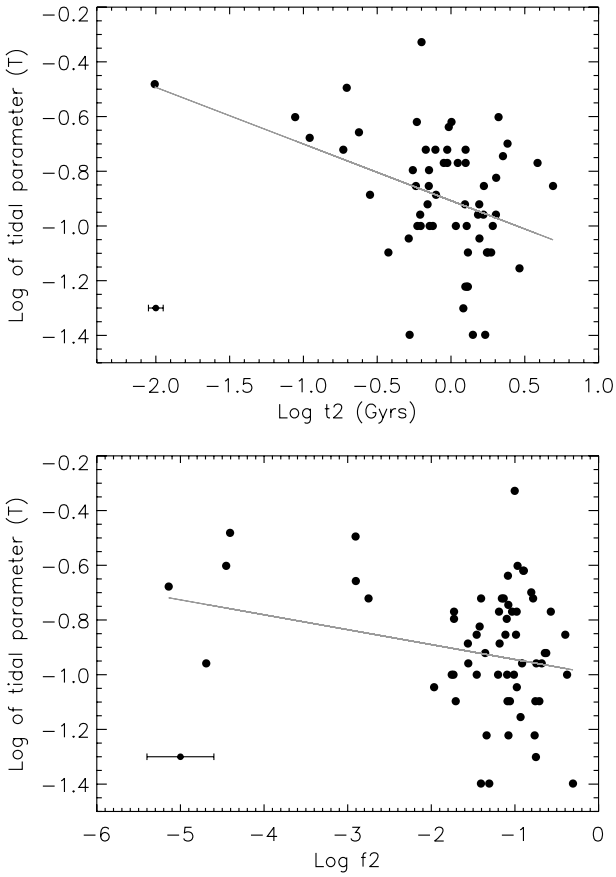

Figure 6. The age (t_2) and mass fraction (f_2) of the recent star formation in the vD05 sample, plotted against the strength of their tidal distortions. Galaxies that have commenced their star formation more recently (i.e. lower values of t_2) show larger tidal distortions. A weak trend also exists between the mass fraction f_2 and the tidal parameter, in the sense that smaller mass fractions correspond to higher values of the tidal parameter.

bottom panel of Fig. 6. Note that the range on the x-axis in this plot is much larger than that in the t_2 versus tidal parameter plot (top panel). Since the tidal features are composed of the underlying stellar mass of the accreted satellite and not the young stars emerging from the starburst (which tend to form preferentially in the central regions of the remnant), the tidal distortion should be relatively insensitive to f_2. However, a residual correlation should be expected, since a larger tidal distortion indicates that the merger is being observed at an earlier stage in the relaxation process. Hence the mass fraction formed is smaller than what it would be if the same remnant was observed later, when the tidal distortion would have decreased and a larger portion of the star formation would have been completed.

The observed trends between colour, t_2, f_2 and tidal distortion can be explained by the fact that galaxies with higher tidal distortions are at an earlier stage in the merger process and the star formation episode that is induced by it. As time passes the remnant relaxes and the star formation activity induced by the merger decreases, as the gas fuelling this process gradually runs out. This results in lower tidal distortions, redder colours and increasing mass fractions, accounting for the trends observed in this study.

We note that our results are in good agreement with the recent study of Sánchez-Blázquez et al. (2009), who studied the vD05 sample using spectral line diagnostics.

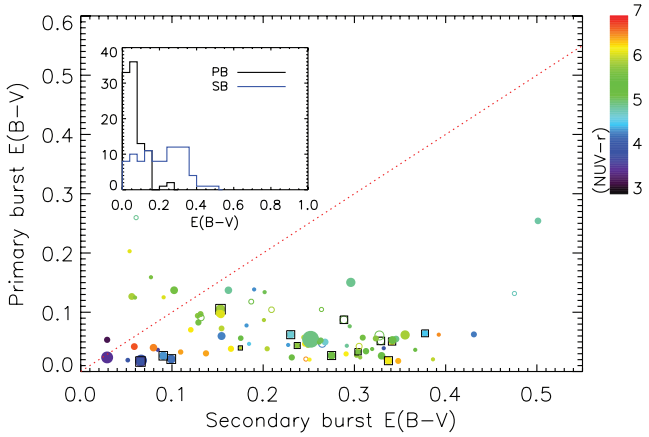

Figure 7. The dust content of the primary burst plotted again the dust content of the secondary burst. The dust extinction of the primary burst (which represents the ISM) is typically less than 0.1, consistent with early types being dust poor. The extinction in star-forming regions is, on average, a factor of 3 higher. Symbol sizes are proportional to the tidality parameter described in Section 2. Galaxies that contain active AGN are shown using open symbols and objects that are currently interacting are indicated using boxes. The galaxies are colour coded based on their (NUV − r) colour.

4.2.2 *Metallicity and dust properties*

The median metallicity values for the galaxies in our sample are in the range 0.8 to 1.4 $Z_{\odot}$, as might be expected for spheroidal galaxies. Recall, from Section 4.1, that a single metallicity is fitted to the entire galaxy, so that the derived metallicity is a representative value for the combined stellar population (old + young) in the galaxy.

In Fig. 7, we present the dust properties of the galaxies in our sample. We find that the ISM extinction in these objects, which is traced by the dust content of the primary burst ($E^{\rm PB}_{B-V}$), is generally less than 0.1, consistent with the expected properties of early-type galaxies as relatively dust-poor systems. In agreement with the findings of Whitaker & van Dokkum (2008), we find that the redness of the vD05 objects is not due to large amounts of dust but simply because the bulk of their stellar populations is old.

While the macroscopic ISM seems to be relatively dust free, we typically derive larger values for $E^{\rm SB}_{B-V}$ (which is representative of the dust in star-forming regions in the galaxy). The bulk of the sample satisfies $E^{\rm SB}_{B-V} < 0.4$. Fig. 7 indicates that the values of $E^{\rm SB}_{B-V}$ can be a few factors larger than $E^{\rm PB}_{B-V}$, which is consistent with the fact that the extinction around star-forming regions (specifically in molecular clouds) is expected to be several times larger than that due to the ISM alone (e.g. Charlot & Fall 2000). The mean value of $E^{\rm PB}_{B-V}/E^{\rm SB}_{B-V}$ is ∼3 [note that the theoretical estimate, for starburst galaxies, derived by Charlot & Fall (2000) is also ∼3]. While $E^{\rm SB}_{B-V}$ applies to only a minority (<10 per cent) of the stellar mass in the galaxy, it is worth noting that the higher extinction appears to affect the second burst even when t_2 is substantially greater than the ages of molecular clouds, which are typically 10–30 Myr (e.g. Blitz & Shu 1980; Hartmann, Ballesteros-Paredes & Bergin 2001). This may indicate that regions of the galaxy where the RSF originates remain dusty. In addition, the parametrization used in this study does not take into account the time-scale over which the RSF takes place (since all bursts are assumed to be instantaneous). In reality, only the youngest stars in the RSF age distribution will probably suffer high extinction but the lack of a time-scale in our analysis leads to the entire second burst suffering higher extinction to account for the plausible effect of molecular clouds.

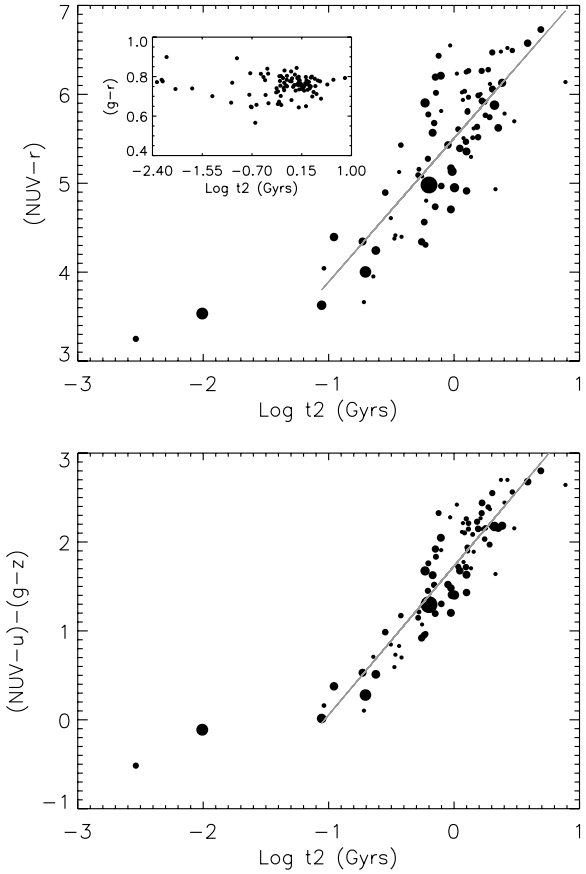

Figure 8. Top: the (NUV − r) colour plotted against the age of the second burst. Bottom: the relatively 'dust insensitive' (NUV − u) − (g − z) double colour plotted against the age of the second burst. The solid line indicates a linear least-squares fit to the relation, which allows us to estimate the age of the last star formation event in early-type galaxies directly from their observed NUV, u, g and z-band photometry.

4.3 A prescription to estimate the age of the last star formation event

The parameter estimation performed in this study allows us to develop a recipe to estimate the age of the most recent star formation event, given the UV and optical photometry of the galaxy in question. We focus on a recipe of the age rather than the mass fraction because the smaller uncertainties in the age make the age estimation significantly more robust.

We note first that the median value for t_2 used in this analysis is extracted from its marginalized PDF, so that the effects of all other parameters (mass fraction, dust and metallicity) have been integrated out. In the top panel of Fig. 8, we plot the median value of t_2 against the (NUV − r) colour. We also show the equivalent plot for the optical (g − r) colour in the inset.

While a clear correlation exists between t_2 and the (NUV − r) colour, there is no equivalent trend with the optical colour. This plot demonstrates both the usefulness of the UV spectrum in quantifying the age of the RSF in early-type galaxies and the insensitivity of the optical spectrum to the residual star formation in these objects.

Although a correlation exists between t_2 and (NUV $-$ r), we note that the (NUV $-$ r) colour is dust sensitive. Standard dust extinction laws (e.g. Cardelli, Clayton & Mathis 1989; Calzetti et al. 2000) indicate that the extinction in the (NUV $-$ r) colour, $A^{\mathrm{NUV}-r} \sim 6E_{B-V}$. Recalling that the estimate for t_2 is marginalized over all other parameters (including dust), we would, ideally, like to compare it to an observational quantity which is also insensitive to dust.

Since the extinctions in colours are linear combinations of the extinctions in the constituent filters, we construct a double colour, (NUV $-$ u) $-$ (g $-$ z), that minimizes the dust sensitivity, given the filter combinations available to us for the bulk of the vD05 sample. The extinction in this colour [assuming a Calzetti et al. (2000) extinction law] is $A^{(\mathrm{NUV}-u)-(g-z)} \sim 1.5E_{B-V}$, a factor of 4 less than that in (NUV $-$ r). Not unexpectedly, plotting t_2 against (NUV $-$ u) $-$ (g $-$ z) produces the same quantitative trend but with less scatter (bottom panel of Fig. 8). The best-fitting line (shown using the solid red line) yields

$$\log t_2\,(\mathrm{Gyrs}) \sim 0.6^{\pm 0.03}[(\mathrm{NUV}-u)-(g-z)-1.73^{\pm 0.03}]. \quad (2)$$

Equation (2) allows us to estimate the age of the last star formation event in early-type galaxies, directly from their observed (i.e. not K-corrected) NUV, u, g and z-band photometry. We note that there appears to be a possible flattening of the slope in the correlation for the very bluest [NUV $-$ r $<$ 3.8 or (NUV $-$ u) $-$ (g $-$ z) $<$ 0] objects (which have been excluded from the fitting above). These objects may obey a different scaling, although the small number of galaxies in this part of the parameter space makes it difficult to derive a robust conclusion. It is possible that, given the very small values of t_2, the star formation activity in these events is in its very early stages, displacing them from the main locus.

5 CONCLUSIONS

We have combined *GALEX* (UV) and SDSS (optical) photometry to derive the recent SFHs of a sample of ∼100 red sequence galaxies, many of which exhibit widespread signs of disturbed morphologies (in deep optical imaging) that are consistent with recent merging events. Originally studied by vD05, more than 70 per cent of bulge-dominated galaxies in this sample show tidal features at a surface brightness limit of $\mu \sim 28\,\mathrm{mag\,arcsec^{-2}}$. An analysis of the spatial (RA, DEC and redshift) distributions of the vD05 objects indicates that the sample is not drawn from overdense regions such as cluster cores and can be considered to be part of the general 'field'. While the vD05 galaxies are optically red, they show a wide dispersion in UV colours that is attributable to low-level RSF, akin to what has been found recently in the general early-type population. Comparison of the vD05 UV colour distribution to that of the general early-type red sequence (drawn from the SDSS) using a KS test indicates that they are drawn from the same parent distribution.

A statistically significant correlation is found between galaxy colour and the intensity of the tidal distortion, in the sense that redder objects show smaller tidal distortions. A stronger trend is observed in the UV colour, since it is more sensitive to low-level recent star formation. Not unexpectedly, a correlation also exists between the parametrized look-back time to the recent star formation event (t_2) and the tidal distortion, in the sense that the tidal distortion decreases with increasing values of t_2. Only a weak trend exists between the mass fraction formed in the event (f_2) and the tidal parameter, with larger values of the tidal parameter corresponding to smaller values of f_2. The observed trends can be explained by the fact that galaxies with higher tidal distortions are at an earlier stage in the merger process and the star formation episode that is induced by it. As time passes the remnant relaxes and the star formation activity decreases, as the gas fuelling this process gradually runs out. This results in lower tidal distortions, redder colours and increasing mass fractions, as found in the trends observed in this study.

The bulk of the vD05 sample has experienced a star formation event in the last 3 Gyrs. The median values of the mass fractions are typically less than 10 per cent. 5 per cent of the sample has experienced a star formation event within the last 0.1 Gyrs and the star formation episodes in these objects appear to be ongoing since the mass fractions formed in these events is very small (<0.1 per cent). If the ongoing mergers in the vD05 sample, that appear to have a median mass ratio of 1:4 (see section 6.2 in vD05), are representative of nearby red mergers, then less than ∼25 per cent of the new stellar mass in the remnants is contributed by star formation. The rest is 'dry accretion' of existing stars. We should note, however, that the large uncertainties on the mass fraction estimates (see Fig. 5) make this statement somewhat uncertain and using the lower limit of the error bars on the f_2 values suggests a lower fraction of less than 10 per cent being contributed by star formation.

The parameter estimation performed in this study allows the primary burst (which takes place at $z = 3$ and contributes the underlying stellar population) and the secondary burst (which represents the most recent burst of star formation and dominates the UV flux) to have different dust extinction values. We find that the dust extinctions in the primary burst (E^{PB}_{B-V}) are typically less than 0.1, consistent with early-type galaxies having ISMs that are dust poor. However, while the macroscopic ISM seems to be relatively dust free, we typically derive larger values for the dust extinction in the second burst (E^{SB}_{B-V}), with the bulk of the sample satisfying $E^{\mathrm{SB}}_{B-V} < 0.4$. The mean value of $E^{\mathrm{SB}}_{B-V}/E^{\mathrm{PB}}_{B-V}$ is ∼3. We note, however, that, while E^{SB}_{B-V} applies to only a minority (<10 per cent) of the stellar mass in the galaxy, the higher extinction appears to affect the second burst even when its age (t_2) is substantially greater than the ages of molecular clouds, which are typically 10–30 Myr. This may indicate that regions of the galaxy where the RSF originates remain dusty. It could also be a result of the parametrization used here, which does not take into account the time-scale over which the RSF takes place (since all bursts are assumed to be instantaneous). In reality, only the youngest stars in the RSF age distribution will probably suffer high extinction but the lack of a time-scale in our analysis leads to the entire second burst suffering higher extinction to account for the plausible effect of molecular clouds.

We have used our analysis to develop a recipe to estimate the age of the most recent star formation event, given the observed UV and optical photometry of the galaxy in question. We find a well-defined correlation between the age of the second burst (t_2), which is marginalized over all other free parameters and the relatively dust-insensitive double colour, (NUV $-$ u) $-$ (g $-$ z). Equation (2) allows us to estimate the look-back time to the last star formation event in red early-type galaxies, directly from their observed (i.e. not K-corrected) NUV, u, g and z-band photometry. The slope in the correlation appears to flatten for the very bluest [NUV $-$ r $<$ 3.8 or (NUV $-$ u) $-$ (g $-$ z) $<$ 0] objects, possibly due to the RSF being ongoing in these systems.

Since the vD05 sample appears to be representative of the general field population of spheroidal galaxies in the nearby Universe (Section 3.2), the results of this study suggest that the widespread low-level star formation that has been reported in nearby spheroidals

is driven by recent mergers. The vast majority of these events do not involve large amounts of gas, indicating that they are either dry major mergers or minor mergers, where the spheroid accretes a small gas-rich satellite (see also Kaviraj et al. 2010). Nevertheless, the spheroidal galaxy population, at present day, is constantly evolving, both dynamically through interaction with companions and in terms of low-level star formation activity induced by these interactions.

ACKNOWLEDGMENTS

I am grateful to the referee for a comprehensive and insightful report which helped strengthen several parts of the paper. I warmly thank Pieter van Dokkum for numerous discussions across several iterations of this paper.

I acknowledge a Research Fellowship from the Royal Commission for the Exhibition of 1851, an Imperial College Research Fellowship and a Senior Research Fellowship from Worcester College, Oxford. Part of this work was supported by a Leverhulme Early-Career Fellowship. Richard Ellis, Sukyoung Yi, Kevin Schawinski and Vandana Desai are thanked for constructive comments.

GALEX is a NASA Small Explorer, launched in 2003 April, developed in cooperation with the Centre National d'Etudes Spatiales of France and the Korean Ministry of Science and Technology.

Funding for the SDSS and SDSS-II has been provided by the Alfred P. Sloan Foundation, the Participating Institutions, the National Science Foundation, the US Department of Energy, the National Aeronautics and Space Administration, the Japanese Monbukagakusho, the Max Planck Society and the Higher Education Funding Council for England. The SDSS Web Site is http://www.sdss.org/.

The SDSS is managed by the Astrophysical Research Consortium for the Participating Institutions. The Participating Institutions are the American Museum of Natural History, Astrophysical Institute Potsdam, University of Basel, University of Cambridge, Case Western Reserve University, University of Chicago, Drexel University, Fermilab, the Institute for Advanced Study, the Japan Participation Group, Johns Hopkins University, the Joint Institute for Nuclear Astrophysics, the Kavli Institute for Particle Astrophysics and Cosmology, the Korean Scientist Group, the Chinese Academy of Sciences (LAMOST), Los Alamos National Laboratory, the Max-Planck-Institute for Astronomy (MPIA), the Max-Planck-Institute for Astrophysics (MPA), New Mexico State University, Ohio State University, University of Pittsburgh, University of Portsmouth, Princeton University, the United States Naval Observatory and the University of Washington.

REFERENCES

Adelman-McCarthy J. K., SDSS collaboration, 2006, ApJS, 162, 38
Baldwin J. A., Phillips M. M., Terlevich R., 1981, PASP, 93, 5
Barnes J. E., Hernquist L., 1992, ARA&A, 30, 705
Bender R., 1997, in Arnaboldi M., Da Costa G. S., Saha P. (eds), ASP Conf. Ser. Vol. 116, The Nature of Elliptical Galaxies. Astron. Soc. Pac., San Francisco, p. 11
Bernardi M., SDSS collaboration, 2003, AJ, 125, 1817
Blitz L., Shu F. H., 1980, ApJ, 238, 148
Bower R. G., Lucey J. R., Ellis R., 1992, MNRAS, 254, 589
Calzetti D., Armus L., Bohlin R. C., Kinney A. L., Koornneef J., Storchi-Bergmann T., 2000, ApJ, 533, 682
Cardelli J. A., Clayton G. C., Mathis J. S., 1989, ApJ, 345, 245
Charlot S., Fall S. M., 2000, ApJ, 539, 718
Chiosi C., Carraro G., 2002, MNRAS, 335, 335
Cole S., Lacey C. G., Baugh C. M., Frenk C. S., 2000, MNRAS, 319, 168
De Lucia G., Springel V., White S. D. M., Croton D., Kauffmann G., 2006, MNRAS, 366, 499
Dressler A., 1980, ApJ, 236, 351
Eggen O. J., Lynden-Bell D., Sandage A. R., 1962, ApJ, 136, 748
Eisenstein D. J. et al., 2001, AJ, 122, 2267
Ellis R. S., Smail I., Dressler A., Couche W. J., Oemler A. J., Butcher H., Sharples R. M., 1997, ApJ, 483, 582
Ferreras I., Silk J., 2000, ApJ, 541, L37
Forbes D. A., Ponman T. J., Brown R. J. N., 1998, ApJ, 508, L43
Franx M., 1993, PASP, 105, 1058
Franx M., 1995, in van der Kruit P. C., Gilmore G., eds, Proc. IAU Symp. 164, Stellar Populations. Kluwer, Dordrecht, p. 269
Gawiser E., MUSYC collaboration, 2006, ApJS, 162, 1
Gladders M. D., Lopez-Cruz O., Yee H. K. C., Kodama T., 1998, ApJ, 501, 571
Hartmann L., Ballesteros-Paredes J., Bergin E. A., 2001, ApJ, 562, 852
Hatton S., Devriendt J. E. G., Ninin S., Bouchet F. R., Guiderdoni B., Vibert D., 2003, MNRAS, 343, 75
Ivezić Ž. et al., 2004, Astron. Nachr., 325, 583
Jannuzi B. T., Dey A., NDWFS Team, 1999, BAAS, 31, 1392
Jorgensen I., Franx M., Kjaergaard P., 1996, MNRAS, 280, 167
Kauffmann G., SDSS collaboration, 2003, MNRAS, 346, 1055
Kauffmann G. et al., 2007, ApJ, 173, 357
Kaviraj S., 2008, Modern Phys. Lett. A, 23, 153
Kaviraj S., Devriendt J. E. G., Ferreras I., Yi S. K., 2005, MNRAS, 360, 60
Kaviraj S., Rey S.-C., Rich R. M., Yoon S.-J., Yi S. K., 2007a, MNRAS, 381, L74
Kaviraj S. et al., 2007b, ApJS, 173, 619 (K07)
Kaviraj S. et al., 2008, MNRAS, 388, 67
Kaviraj S. et al., 2009, MNRAS, 394, 1713
Kaviraj S., Tan K., Ellis R. S., Silk J., 2010, preprint (arXiv:1001.2141)
Larson R. B., 1974, MNRAS, 166, 385
Mapelli M., Sigurdsson S., Ferraro F. R., Colpi M., Possenti A., Lanzoni B., 2006, MNRAS, 373, 361
Maraston C., Strömbäck G., Thomas D., Wake D. A., Nichol R. C., 2009, MNRAS, 394, L107
Martin D. C., GALEX collaboration, 2005, ApJ, 619, L1
Mason K. O. et al., 2001, A&A, 365, L36
Mochkovitch R., 1986, A&A, 157, 311
Morrissey P. et al., 2007, ApJS, 173, 682
Muzzin A., Marchesini D., van Dokkum P. G., Labbé I., Kriek M., Franx M., 2009, ApJ, 701, 1839
Peebles P. J. E., 2002, in Metcalfe N., Shanks T. (eds), ASP Conf. Ser. Vol. 283, A New Era in Cosmology. Astron. Soc. Pac., San Francisco, p. 351
Peirani S., Crockett R. M., Green S., Khochfar S., Kaviraj S., Silk J., 2010, MNRAS, 405, 2327
Saglia R. P., Colless M., Baggley G., Bertschinger E., Burstein D., Davies R. L., McMahan R. K., Wegner G., 1997, in Arnaboldi M., Da Costa G. S., Saha P., eds, ASP Conf. Ser. Vol. 116, The Nature of Elliptical Galaxies. Astron. Soc. Pac., San Francisco, p. 180
Salim S., GALEX collaboration, 2007, ApJS, 173, 267
Sánchez-Blázquez P., Gibson B. K., Kawata D., Cardiel N., Balcells M., 2009, MNRAS, 400, 1264
Schawinski K. et al., 2007a, ApJS, 173, 512
Schawinski K., Thomas D., Sarzi M., Maraston C., Kaviraj S., Joo S.-J., Yi S. K., Silk J., 2007b, MNRAS, 382, 1415
Stanford S. A., Eisenhardt P. R. M., Dickinson M., 1998, ApJ, 492, 461
Stasińska G., Vale Asari N., Cid Fernandes R., Gomes J. M., Schlickmann M., Mateus A., Schoenell W., Sodré L., Jr, 2008, MNRAS, 391, L29
Thomas D., Greggio L., Bender R., 1999, MNRAS, 302, 537
Toomre A., 1977, in Tinsley B. M., Larson R. B., eds, Evolution of Galaxies and Stellar Populations. Yale Univ. Observatory, p. 401

van Dokkum P. G., 2005, AJ, 130, 2647 (vD05)
van Dokkum P. G., Franx M., 1996, MNRAS, 281, 985
van Dokkum P. G., Franx M., Fabricant D., Illingworth G. D., Kelson D. D., 2000, ApJ, 541, 95
van Dokkum P. G. et al., 2010, ApJ, 709, 1018
Wall J. V., 1996, QJRAS, 37, 519
Wheeler J. C., 1979, ApJ, 234, 569
Whitaker K. E., van Dokkum P. G., 2008, ApJ, 676, L105
Worthey G., 1994, ApJS, 95, 107
Yi S. K., 2003, ApJ, 582, 202
Yi S., Demarque P., Oemler A. J., 1997, ApJ, 486, 201
Yi S., Lee Y.-W., Woo J.-H., Park J.-H., Demarque P., Oemler A. J., 1999, ApJ, 513, 128
Yi S. K., Yoon S.-J., Kaviraj S., Deharveng J.-M., GALEX Science Team, 2005, ApJ, 619, L111
York D. G., SDSS collaboration, 2000, AJ, 120, 1579

This paper has been typeset from a TEX/LATEX file prepared by the author.